

Study of a Lattice-Gas Hamiltonian for Micellar Binary Solutions

Abdelilah Benyoussef and Najem Moussa
LMPHE Faculté des Sciences, B.P. 1014, Rabat, Morocco.

Lahoussine Laanait
Ecole Normale Supérieure, B.P. 5118, Rabat, Morocco.

Nouredine Masaif
LM Faculté des Sciences et Techniques B.P. 577, Settat, Morocco

We have study the low temperature phase diagram of a lattice model of the micellar binary solutions (MBS) of water and amphiphile. The mean field approximation is used to investigate the phase diagrams of the micellar binary solutions in the presence of a chemical potential of the amphiphiles for different values of coupling interactions. New phases appear between water-rich and amphiphile-rich. Second and first order transitions, tricritical, multicritical and critical end-points are obtained. By a simple low temperature expansion argument, we have confirmed the states of lowest free energy in a mean field approximation.

PACS number (s): 75.10 b

I. INTRODUCTION

In recent years great effort has been made in experimental and theoretical physics to understand the behavior of phase diagrams of amphiphilic systems.

Recently, several models of the binary mixtures of amphiphile (it is a molecule of both hydrophilic and hydrophobic parts) and water have been proposed in order to reproduce the phases observed experimentally¹⁻⁷.

In general, the amphiphile molecules in the mixtures water-amphiphile try to arrange themselves as to only expose their polar head groups to the water molecules. In particular, when the amphiphile wholly immersed in water, the molecules again try to reduce the area of contact with water in order to form the following aggregates (rods, spheres, lamellar, ...). Precisely, when a hydrocarbon is in contact with water, the network of hydrogen bonds between water molecules reconstructs itself to avoid the region occupied by hydrocarbon. This constraint on the local structure of water decreases the entropy near the hydrocarbon, and it results in an increasing of the free energy of the system⁸. The extensive application of light and neutron scattering and nuclear magnetic resonance has produced a wealth of important experimental results which agree with what is said above³.

For amphiphilic systems, the aggregation of molecules of the binary solution induces equilibrium processes controlled by intermolecular and interaggregate forces⁹. Micellar aggregates appear in various shapes and sizes, depending on the amphiphiles, the concentration and other thermodynamic parameters. This suggests a classification of the aggregates into three general categories as follows: 1-Globular aggregates where a spherical micelle is a prototype of this class. 2- Rod-like aggregates where a cylindrical micelle is the typical example of this class. 3- Bilayers where disk-like aggregate is a example of this class. The choice among all the possible shapes is

determined by interactions between the hydrophilic headgroups and geometric packing constraints on the hydrophobic tails, but the transition from one shape to another may be obtained by changing either the temperature or the concentration or by adding a third component.

With increasing amphiphile concentration a variety of lyotropic phases are found (see 9-14). The phase diagram for the system water and $C_{12}E_5$ (i.e $C_{12}H_{25}(OC_2CH_2)_5 OH$) is reproduced by Streyl et al¹³ representing such phenomena.

At low temperatures, Gompper-Schick⁴ and Matsen-Sullivan³ have exhibit within mean field theory a two phase coexistence between homogeneous water-rich and amphiphile-rich phases. But at higher temperatures, there is a single disordered phase. The phase diagram established in⁴ resembles that of the system $C_{12}E_5$ and water⁹ for which scattering experiments have carried out¹⁴.

II. TWO DIMENSIONAL SCHNIDMANN-ZIA MODEL

Concerning the microscopic approach, Shnidman and Zia¹⁶ recently proposed a lattice-gas model, based on constructing a coarse-grained representation of different types of aggregates occurring in micellar binary solutions (MBS's) in terms of Ising variables. Namely, one introduces on a lattice site (i,j) the Ising variable satisfying $s_{i,j}=+1$ for a micellar section and $s_{i,j}=-1$ describes a region, of comparable size, predominantly occupied by a solvent. A single +1 spin completely surrounded by -1 spins is identified with a globular micelle, and a linear chain of +1 spins surrounded by -1 spins corresponds to a rod-like micelle. Finally, a spin +1 at the end of a chain of +1 spins surrounded by -1 spins is called an end cap (see Ref. 16). The Hamiltonian of the proposed model is a sum of three terms:

$$H = H_K + H_J + H_h,$$

where H_K is effective at the intramolecular length scale, representing many-body interactions responsible for self-association and controlling the size and shape distribution of aggregates, and H_J describes an effective short-range coupling between the aggregates at larger intermicellar length scale. Finally, H_h is the part controlling the concentration of aggregates.

We assign negative energies $-K_0$ and $-K_1$, respectively, for the formation of a spherical micelle and a rodlike micelle. For an end-cap, the average $-(K_0+K_1)/2$ is chosen.

To write H explicitly, it is convenient to use the lattice-gas variables

$$t_{i,j} = (1 + \sigma_{i,j}) / 2 \quad \text{and} \quad S_{i,j} = (1 - \sigma_{i,j}) / 2.$$

For further convenience, we define the bilinear products

$$u_{j,j} = t_{i-1,j} t_{i+1,j}$$

$$v_{j,j} = S_{i-1,j} S_{i+1,j}$$

$$w_{j,j} = t_{i-1,j} S_{i+1,j} + S_{i-1,j} t_{i+1,j}$$

and similar ones with $i \leftrightarrow j$. In terms of these operators, H is

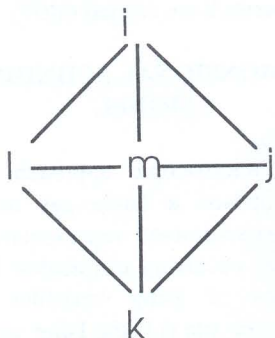
$$H = -K_0 \sum t_{ij} v_j - \frac{1}{2} (K_0 + K_1) \sum t(w_{ij} v_j + v_j w_{ij}) - K_1 \sum t(u_{ij} v_j + v_i u_j) - J \sum S(u_{ij} + v_j) - h \sum S(t-s) \quad (1)$$

where we have suppressed all except the underlined indices and the summations are over all site indices¹⁶.

The Hamiltonian H is transformed in terms of Ising variables, into the form

$$\begin{aligned} -H = & J_1 \sum_{(1)} \sigma_i + J_2 \sum_{(2)} \sigma_i \sigma_j + J_3 \sum_{(3)} \sigma_i \sigma_j + J_4 \sum_{(4)} \sigma_i \sigma_j \\ & + J_5 \sum_{(5)} \sigma_i \sigma_j \sigma_k + J_6 \sum_{(6)} \sigma_i \sigma_j \sigma_k + J_7 \sum_{(7)} \sigma_i \sigma_j \sigma_k \\ & + J_8 \sum_{(8)} \sigma_i \sigma_j \sigma_k \sigma_l + J_9 \sum_{(9)} \sigma_i \sigma_j \sigma_k \sigma_l \\ & + J_{10} \sum_{(10)} \sigma_i \sigma_j \sigma_k \sigma_l \sigma_m \end{aligned} \quad (2)$$

The sum runs over all the spins in different sites, bonds and loops on the following cell:



and $J_1 = (-5K_0 + 8J + 32h)/32$, $J_2 = (-4K_0 + 2K_1 + 8J)/32$, $J_3 = (-2K_0 - 4K_1)/32$, $J_4 = -(K_0 + 2K_1 + 4J)/32$, $J_5 = (K_0 + 2K_1 - 4J)/32$, $J_6 = (K_0 - 2K_1)/32$, $J_7 = J = K_1/32$, $J_8 = J_9 = J_{10} = -K_0/32$,

where K_0 , K_1 and J are positive. We notice that the model describing the physical situation corresponds to positive values of J .

A. Low temperature analysis

Our aim in this section is to propose a description of the ground states of the model and to describe the low temperature phase diagrams in dimension 2 for certain values of the parameters K_0 , K_1 , J and h .

1. Ground states of the model

To describe the ground states of the model we define a covering of the lattice by lozenges, L , such that $H = \sum_L e_L$.

$$\begin{aligned} & \sigma_2 \\ \text{and } L \equiv & \sigma_3 \quad \sigma_0 \quad \sigma_1 \\ & \sigma_4 \end{aligned}$$

The different configurations of lozenges and their energies, calculated from equation (2), are :

+	-	+	+	+	+	+	+	+
+	-	+	+	+	+	+	+	+
L_1	+	L_2	+	L_3	+	$e_1 = -3J_1/5 - 8K_0 - 4K_1 - 32J$	$e_2 = -3J_1/5 + 2K_0 + 6K_1 + 8J$	$e_3 = -J_1 - 2K_0 + 4K_1 + 16J$
-	-	-	+	-	+	+	+	-
L_4	-	L_5	+	L_6	+	$e_4 = J_1 + 8K_0 + 4K_1$	$e_5 = -J_1/5 - 4K_0 - 2K_1 - 8J$	$e_6 = -h/5 + 6K_0 + 8K_1$
-	-	-	+	-	-	-	+	-
L_7	-	L_8	+	L_9	+	$e_7 = -J_1/5 + 6K_0 - 24K_1$	$e_8 = J_1/5 - 16J$	$e_9 = J_1/5 + 16J$
+	+	+	-	-	-	+	-	-
-	+	-	-	-	-	-	+	-
L_{10}	-	L_{11}	-	L_{12}	-	$e_{10} = J_1/5 - 6K_0 - 6K_1 - 8J$	$e_{11} = 3J_1/5 + 4K_0 + 2K_1 + 8J$	$e_{12} = 3J_1/5 - 18K_0 + 12K_1 - 16J$

We notice that for a given configuration of lozenges its symmetricals by the rotation symmetry have the same energy.

In order to obtain the ground states (By a ground state of the system we will understand a configuration which is periodic and for which the energy e_0 per lattice site is minimal) we first propose to classify the energies e_1, e_2, \dots, e_{12} . The minimum depends on the values of the parameters K_0, K_1, J and h . After having found the minimum of e_1, e_2, \dots, e_{12} we choose to class them in an increasing order. Then we searched for the covering of the lattice by a subset of lozenges L_1, L_2, \dots, L_{12} , which leads to a ground state.

In order to discuss the phase diagrams of this model, it is useful to introduce the ground states of the system which are defined as follows:

We denote by G_1 the water ground state (g.s), G_2 the spherical micelles (g.s), G_3 the rarefied spherical micelles (g.s), G_4 the infinite rodlike micelles (g.s), G_5 the reversed micelles (g.s) and G_6 the amphiphile (g.s) (see Fig. 1a).

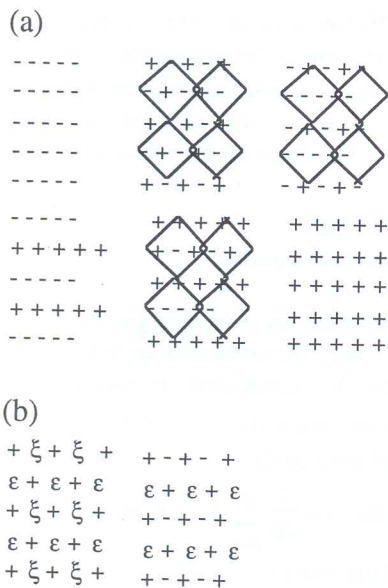


FIG. 1. (a) Ground states: G_1 , the water ground state (g.s); G_2 , the spherical micelles (g.s); G_3 , the rarefied spherical micelles (g.s); G_4 , the infinite rodlike micelles (g.s); G_5 , the reversed micelles (g.s) and G_6 , the amphiphile (g.s). (b) The configurations with residual entropy of G_5 : the spins ϵ may take indifferently the value +1 or -1. (b) The configurations with residual entropy of G_2 are governed by the following constraints: If $\xi = -1$, then the next-nearest neighbors (NNN's) (ϵ) of the spin ξ can take indifferently the value +1 or -1. If $\xi = +1$, all the NNN's of the spin ξ must take the value -1 (From Ref. 17).

Their energies, calculated from equation (2), are the following :

$$\begin{aligned} \epsilon_0(G_1) &= h, & \epsilon_0(G_2) &= -(K_0 + 2J)/2, & \epsilon_0(G_3) &= (-2h + K_0 + 2J)/4, \\ \epsilon_0(G_4) &= -(2K_0 + K_1 + 4J)/6, & \epsilon_0(G_5) &= -(K_0 + K_1 + 2J)/4, \\ \epsilon_0(G_6) &= -h \end{aligned} \quad (4)$$

The phase diagram at zero temperature for different values of the parameters, K_0 , K_1 and J present five regions: (1) $K_1 > K_0$ and $J < K_1 - K_0$, (2) $K_1 > K_0$ and $0 < J < K_1 - K_0$, (3) $K_0/2 < K_1 < K_0$ and $J > 0$, (4) $K_1 > K_0/2$ and $J > 0$, (5) $K_1 < K_0$ and $J = K_1 - K_0$ (see Fig. 2 and Ref. 18).

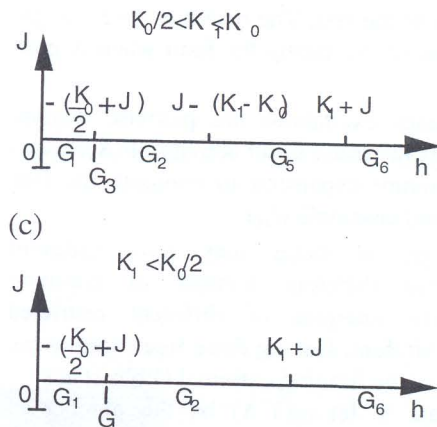
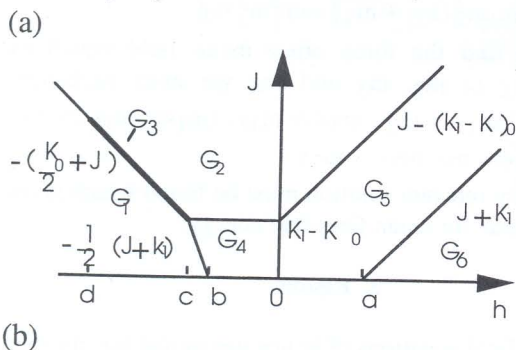


FIG. 2. (a) The phase diagrams at zero temperature in the space of the parameters J , h , with $K_1 > K_0$. The points a, b, c, and d correspond to $K_1, -K_1/2, -(2K_1 - K_0)/2$ and $-(4K_1 - 3K_0)/2$ respectively. (b) The zero temperature phase diagram for the case where $K_1/2 < K_1 < K_0$. (c) The zero temperature phase diagram for the case where $K_1 < K_0/2$.

2. The low temperature phase diagrams

The analysis we propose is a direct application of the theory of first order phase transition performed by Pirogov and Sinai¹⁹ and formulated by Slawny²⁰.

We first need to introduce the notion of elementary excitations²¹. By an excitation we understand a configuration which coincides with a ground state outside of a finite set of sites.

If X is a local excitation of a ground state Y , i.e., X is equal to Y outside of a finite set, then $H(X|Y)$ will denote its energy with respect to Y . Let e be the set of all the excitation energies :

$$e = \{H(X|Y) / X \text{ is a local excitation of } Y\}, e = \{0, E_1, E_2, \dots\}.$$

In our case we observe that the energy of an excitation (relative to the corresponding ground state) tends to infinity with the size of the region where it differs from the ground state and then the Peierls condition needed in the Pirogov and Sinai theory is satisfied for the 2- dimensional model. Therefore we pay a particular attention to the elementary excitations X , corresponding to change the configuration of only one site in a given ground state (see Table 1 in Ref. 17) and the energy, $E(X)$, relative to the ground state is defined as the energy of the configuration X minus the energy of the ground state.

If Y is a configuration of the system equal to a ground state configuration outside a finite large box Λ we verify that there exist a uniquely defined configuration obtained from Y by removing all elementary excitations with energy $E(X)$ less than E_n .

We define the set, $e(Y, E_n)$, to be the restricted ensemble of configurations of elementary excitations with energy less than E_n .

The restricted partition function, Z_R , of the configuration of the set $e(Y, E_n)$, is obtained by assigning to every configuration of the set $e(Y, E_n)$, its Boltzmann weight and

give zero probability to the rest. The restricted free energy, f_R , is obtained, as usual, by taking the limit when Λ goes to infinity.

Since the elementary excitations are pairwise disjoint support then one uses the usual small activity, $\Phi(X) = \text{Exp}(-\beta E(X))$, low temperature expansion to compute the free energy of the restricted ensemble (f_R).

Since different ground states may have different excitations and also different number of common excitations, the free energies of different restricted ensembles may be different. Having these free energies we discuss the stability of the limiting extremal Gibbs states.

For a ground state Y let $n_i(Y, \Lambda)$ be the number of excitations of Y in the box Λ with energy E_i and Z_Λ^Y the partition function of the system in Λ with Y boundary conditions. For low enough temperatures we have :

$$\frac{1}{\Lambda} \log Z_\Lambda^Y = n_0(Y, \Lambda) \beta \epsilon_0 + n_1(Y, \Lambda) e^{-\beta E_1} + n_2(Y, \Lambda) e^{-\beta E_2} + \dots \quad (5)$$

The multiplicities are the limits of the coefficients of this expansion as Λ becomes large :

$$n_i(Y) = \lim_{\Lambda \rightarrow \infty} n_i(Y, \Lambda) \quad (6)$$

Then the free energy $f(\beta)$ has the following asymptotic expansion as $T \rightarrow 0$:

$$f(\beta) = \beta \epsilon_0 + n_1 e^{-\beta E_1} + n_2 e^{-\beta E_2} + \dots + n_k e^{-\beta E_k} + \dots \quad (7)$$

To describe the low temperature phase diagram we need to consider instead of G_2 and G_5 certain restricted ensembles of configurations in which we define, by introducing the Ising variables ϵ and ξ (Fig. 1b) the sets :
- \bar{G}_2 the set of configurations satisfying to the constraint :
if $\xi = -1$ then the next nearest neighbors (NNN)(ϵ) of ξ can take indifferently $+1$ or -1 but when $\xi = +1$, all the (NNN) take only the value -1 . The excitations energies of \bar{G}_2 are given in table 2 (see Ref. 17).

B. Mean-field approximation

In this section we present the phase diagram of the micellar binary solutions in dimension 2 in the space of the parameters J and h (chemical potential of the amphiphiles) for values competing interactions satisfying the condition $K_1 > K_0$. So, for the fixed values of h which are well chosen in an interval given, we propose a description within the mean-field approximation of phase diagrams in the (T, J) plan where T is the temperature.

Our first motivation for this study was the well-known fact that the parameter J for the fixed values of the chemical potential of the amphiphiles, h , may change the nature of the phase transitions in a fundamental way, inducing the appearance of the critical end-points, tricritical and multicritical points. Second, to verify that the model proposed by Shnidman and Zia describe very well the micellar solutions.

For different values of the parameters, J , with $K_1 > K_0$, we established the phase diagram at zero temperature in the

space of the parameters J and h (see Fig. 2a). This phase diagram indicated all ground states which are defined previously.

To characterize the different ground states, in the mean field approximation, we introduce the parameters m_i , ($i=1, \dots, 4$) corresponding to four magnetizations on the four sublattices. Hence, for example, the rarefied spherical micelles ground state can be specified by $(m_1 = -1, m_2 = -1, m_3 = -1, m_4 = +1)$.

1. Mean field equations

In mean field approximation the free energy, F , of the micellar binary solutions may be expressed as function of the inverse temperature β , variational parameters h_i , $i=1, \dots, 4$, the magnetizations m_i , $i=1, \dots, 4$, and h_i , $i=1, \dots, 10$, which are mentioned previously:

$$F = -\frac{1}{4\beta} \sum_{i=1}^4 \log 2 (\cosh(\beta h_i)) + \frac{1}{4\beta} \sum_{i=1}^4 (h_i - J_1) m_i - (J_2 / 2) (m_1 + m_4) (m_2 + m_3) - J_3 (m_1 m_4 + m_2 m_3) - (J_4 / 2) (m_1^2 + m_2^2 + m_3^2 + m_4^2) - (J_5 / 4) ((m_1 + m_4) (m_2^2 + m_3^2) + (m_2 + m_3) (m_1^2 + m_4^2)) - J_6 (m_1 m_2 (m_3 + m_4) + m_3 m_4 (m_1 + m_2)) - J_7 (m_1 m_4 (m_1 + m_4) + m_2 m_3 (m_2 + m_3)) - (J_8 / 2) (m_1 m_4 + m_2 m_3) (m_1 + m_4) (m_2 + m_3) - (J_9 / 2) (m_1^2 m_4^2 + m_2^2 m_3^2) - (J_{10} / 2) (m_1^2 m_4^2 (m_2 + m_3) + m_2^2 m_3^2 (m_1 + m_4)) \quad (8)$$

where the function m_i , $i=1, \dots, 4$, that is the average magnetization per spin, is given as follows:

$$m_i = \tanh(\beta h_i)$$

The mean field equations in this situation are obtained by minimizing the expression of free energy, F , with respect to the variational parameters m_i , $i=1, \dots, 4$, which combined with the last expression of magnetization. Then the first equation of this system corresponding to m_1 is:

$$m_1 = \tanh\{\beta(J_1 + 2J_2(m_2 + m_3) + 4J_3 m_4 + 4J_4 m_1 + J_5(2m_1(m_2 + m_3) + (m_2^2 + m_3^2)) + 4J_6(m_3 m_4 + m_2(m_3 + m_4)) + 4J_7(2m_1 m_4 + m_4^2) + 4J_9 m_1 m_4^2 + 2J_8(m_2 + m_3)(2m_1 m_4 + m_2 m_3 + m_4^2) + J_{10}(2m_1 m_4^2(m_2 + m_3) + m_2^2 m_3^2))\} \quad (9)$$

In order to find the three other mean field equations corresponding to m_2 , m_3 and m_4 we must exchange, respectively, $(m_1 \leftrightarrow m_2, m_3 \leftrightarrow m_4)$, $(m_1 \leftrightarrow m_3, m_2 \leftrightarrow m_4)$ and $(m_1 \leftrightarrow m_4, m_2 \leftrightarrow m_3)$.

The physically relevant solution must be found which gives the lowest value for mean field free energy.

2. Results

The mean field equations of lattice gas model for micellar binary solutions give different regions of the phase

diagrams where the phase transition lines and the multicritical points, especially critical and tricritical points, are indicated.

In order to realize this, we construct T-J phase diagrams, which exhibit a variety of phases, for various values of the chemical potential of the amphiphiles, h . So, to describe the behaviour appearing in the phase diagrams, we define, $L(i,j)$, as the phase transition line that possesses i and j as extremities and, $L(i,\infty)$, if j as an infinite extremity.

Following Griffiths²², we define the points: $-B^m A^n$ as the critical end-point which is the intersection of m lines of second order and n lines of first order; $-B^m$ multicritical point (which is the intersection of m lines of second order);

$-A^n$ the n -phase point (where n which is the intersection of n lines of the first order). In particular we call C the tricritical point which is the intersection of a line of second order and a line of first order. Here we give the pertinent cases only.

In the case $h \in [-(1/2)(4K_1 - 3K_0), -(1/2)(2K_1 - K_0)]$ (here we choose, for example, $K_1/K_0 = 2$ and $h/K_0 = -2$), the phase diagram represent the following phases corresponding to G_1 , G_2 and G_3 . We distinguish that the triple point A^3 separates the phase transition lines $L(3, A^3)$ and $L(A^3, C)$ of the first order transitions. The tricritical point C separates the phase transition lines $L(A^3, C)$ of the first order transition from one $L(C, \infty)$ of the second-order transition (Fig. 3).

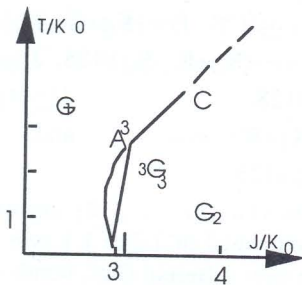


FIG. 3. Phase diagram of the model for $h \in [-(1/2)(4K_1 - 3K_0), -(1/2)(2K_1 - K_0)]$ (for example, $K_1/K_0 = 2$ and $h/K_0 = -2$) on the T-J plane. G_1 , G_2 and G_3 are different pure phases. The solid lines are first order transitions and the dashed lines are second-order transitions. The triple point A^3 and the tricritical point C occur.

In the case $h \in [-K_1/2, 0]$ (here we choose, for example, $K_1/K_0 = 2$ and $h/K_0 = -0.5$), the phase diagram represents the following phases corresponding to G_1 , G_2 , G_3 , G_4 and G_5 .

The critical end-points $(BA^2)_1$, $(BA^2)_2$ and B^2A separate the phase transition lines $L(1.9, (BA^2)_1)$, $L((BA^2)_1, (BA^2)_2)$, $L((BA^2)_2, 2.)$ and $L(2.1, B^2A)$ of the first order transitions from ones $L((BA^2)_1, B^2A)$,

$L((BA^2)_2, B^3)$ and $L(B^2A, B^3)$ of the second-order transition. The multicritical point B^3 separates the phase transition lines $L((BA^2)_2, B^3)$, $L(B^2A, B^3)$ and $L(B^3, \infty)$ of the second-order transitions (Fig. 4).

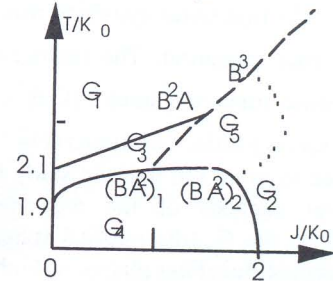


FIG. 4. Phase diagram of the model for $h \in [-K_1/2, 0]$ (for example, $K_1/K_0 = 2$ and $h/K_0 = -0.5$) on the T-J plane. G_2 and G_4 are pure phases. The solid lines are first order transitions and the dashed lines are second-order transitions. The critical end-points $(BA^2)_1$ and $(BA^2)_2$ and the multicritical points B^3 occur.

In the case $h = 0$ (here we choose, for example, $K_1/K_0 = 2$ and $h/K_0 = 0$) on the T-J plane, the phase diagram represents the following phases corresponding to G_1 , \bar{G}_2 and \bar{G}_5 , namely:

$-\bar{G}_2$ is the state with residual entropy (Fig. 1b) corresponding to G_2 . Here we identified this phase by observing the four sublattices magnetizations (m_1, m_2, m_3, m_4) such that $m_1 > 0$, $m_2 < 0$, $m_3 < 0$ and $m_4 > 0$ where the sublattices corresponding to m_1 and m_4 (resp. m_2 and m_3) are equivalent (resp. non-equivalent).

$-\bar{G}_5$ is the state with residual entropy (fig. 1b) corresponding to G_5 . We note that this phase is characterised, in the mean field case, by the disappearance of the magnetization in some sublattice at $J = h + K_1 - K_0$ (e.g. $J = 2.$). For $J < h + K_1 - K_0$ (e.g. $J < 2.$), the magnetization on this sublattice increases continuously from 0 to +1 while J decreases.

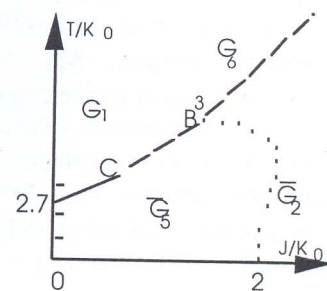


FIG. 5. Phase diagram of the model for $h = 0$ (for example, $K_1/K_0 = 2$ and $h/K_0 = 0$) on the T-J plane. \bar{G}_2 and \bar{G}_5 are pure phases. The solid lines are first order transitions and the dashed lines are second-order transitions. The tricritical point C and the multicritical points B^3 occur.

We point out that although there is a coexistence of two ground states G_4 and G_5 at zero temperature for $0 < J < K_1 - K_0$, only one phase appears at non-zero temperatures. Beside, the tricritical point C separates the phase transition lines $L(2.7, C)$ of the first order transition from one $L(C, B^3)$ of the second-order transition. The multicritical point B^3 separates the phase transition lines $L(C, B^3)$, $L(2., B^3)$ and $L(B^3, \infty)$ of the second-order transitions (Fig.5).

We would like to point out that the study by means of a direct numerical analysis of the mean-field equations allows to establish the G_3 (the rarefied spherical micelles) and G_5 (the reversed micelles) phases at high temperatures and which disappear at low temperatures.

III. THREE DIMENSIONAL SCHNIDMANN-ZIA MODEL

To write explicitly the Hamiltonian proposed in three dimensional, it is convenient to use the lattice-gas variables $t_{i,j,k} = (1 + \sigma_{i,j,k})/2$ and $\tilde{t}_{i,j,k} = (1 - \sigma_{i,j,k})/2$.

For further convenience, we define the bilinear products

$$u_{i,j,k} = t_{i-1,j,k} t_{i+1,j,k}$$

$$\tilde{u}_{i,j,k} = \tilde{t}_{i-1,j,k} \tilde{t}_{i+1,j,k}$$

$$w_{i,j,k} = t_{i-1,j,k} \tilde{t}_{i+1,j,k} + \tilde{t}_{i-1,j,k} t_{i+1,j,k},$$

and similar ones obtained by changing i into j and i into k .

In terms of these operators, H is

$$\begin{aligned} H = & -K_0 \sum \tilde{u}_j \tilde{u}_j \tilde{u}_k - \frac{1}{2} (K_0 + K_1) \sum t(w_j \tilde{u}_j \tilde{u}_k \\ & + \tilde{u}_j w_j \tilde{u}_k + \tilde{u}_j \tilde{u}_j w_k) - \frac{1}{2} (K_1 + K_2) \\ & \sum t(u_j w_j \tilde{u}_k + w_j u_j \tilde{u}_k + \tilde{u}_j w_j u_k) \\ & + \tilde{u}_j u_j w_k + w_j \tilde{u}_j u_k + u_j \tilde{u}_j w_k) \\ & - K_1 \sum t(u_j \tilde{u}_j \tilde{u}_k + \tilde{u}_j u_j \tilde{u}_k + \tilde{u}_j \tilde{u}_j u_k) \\ & - K_2 \sum t(u_j u_j \tilde{u}_k + \tilde{u}_j u_j u_k + u_j \tilde{u}_j u_k) \\ & - J \sum \tilde{t}(u_j + u_j + u_k) - h \sum (t - \tilde{t}) \end{aligned} \quad (10)$$

where we have suppressed all except the underlined indices and the summations are over all site indices¹⁶.

We assign negative energies $-K_0$, $-K_1$ and $-K_2$, respectively, for the formation of a spherical micelle, a rod-like micelle and a layer-like micelle (planes of $+1$ spins surrounded by -1 spins). For simplicity, we give the configurations of these energies in a two dimensional system¹⁶. For an end-caps "spherical-rodlike", "rodlike-layer", the averages $-(K_0 + K_1)/2$ and $-(K_1 + K_2)/2$ is chosen respectively.

To have an idea of the dependence of the energies $-K_0$, $-K_1$ and $-K_2$ and the characteristics of the amphiphile molecule, let l and v denote, respectively, the length and the volume of the molecule. let also a be the area of the head-group of the molecule. Then if $a < 3(v/l)$ the amphiphiles prefers to organize in spherical micelles⁶ and

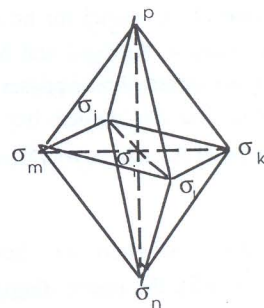
then the energy $-K_0$ is less than the others energies ($-K_1$ and $-K_2$). If now $2(v/l) < a < 3(v/l)$ the spherical micelles are unstable and the rod-like micelles are the preferred micellar geometry and then $-K_0$ is less than the others energies ($-K_1$ and $-K_2$). Finally, if $(v/l) < a < 2(v/l)$ the layer-like is the only stable aggregation geometry (among the three basic shapes considered); so $-K_2$ is less than the others energies ($-K_0$ and $-K_1$).

The Hamiltonian H is transformed in terms of Ising variables, to the form

$$\begin{aligned} -H = & J_1 \sum_{(1)} \sigma_i + 2J_2 \sum_{(2)} \sigma_i \sigma_j + 2J_3 \sum_{(3)} \sigma_i \sigma_j \\ & + J_4 \sum_{(4)} \sigma_i \sigma_j + J_5 \sum_{(5)} \sigma_i \sigma_j \sigma_k + J_6 \sum_{(6)} \sigma_i \sigma_j \sigma_k \\ & + J_7 \sum_{(7)} \sigma_i \sigma_j \sigma_k + J_8 \sum_{(8)} \sigma_i \sigma_j \sigma_k + J_9 \sum_{(9)} \sigma_i \sigma_j \sigma_k \sigma_l \\ & + J_{10} \sum_{(10)} \sigma_i \sigma_j \sigma_k \sigma_l + J_{11} \sum_{(11)} \sigma_i \sigma_j \sigma_k \sigma_l \\ & + J_{12} \sum_{(12)} \sigma_i \sigma_j \sigma_k \sigma_l + J_{13} \sum_{(13)} \sigma_i \sigma_j \sigma_k \sigma_l \sigma_m \\ & + J_{14} \sum_{(14)} \sigma_i \sigma_j \sigma_k \sigma_l \sigma_m + J_{15} \sum_{(15)} \sigma_i \sigma_j \sigma_k \sigma_l \sigma_m \\ & + J_{16} \sum_{(16)} \sigma_i \sigma_j \sigma_k \sigma_l \sigma_m \sigma_n + J_{17} \sum_{(16)} \sigma_i \sigma_j \sigma_k \sigma_l \sigma_m \sigma_n \\ & + J_{18} \sum_{(18)} \sigma_i \sigma_j \sigma_k \sigma_l \sigma_m \sigma_n \sigma_p \end{aligned} \quad (11)$$

where $J_1 = h - ((14K_0 + 6K_1 - 15K_2 - 48J)/128)$, $J_2 = -(6K_0 + 6K_1 - 2K_2 - 32J)/128$, $J_3 = -(4K_0 + 4K_1 + 6K_2)/128$, $J_4 = -(2K_0 + 6K_1 + 5K_2 + 16J)/128$, $J_5 = (2K_0 + 6K_1 + 5K_2 - 16J)/128$, $J_6 = (2K_0 - 2K_1 - 3K_2)/128$, $J_7 = -(K_0 + K_1 - K_2)/128$, $J_8 = -(K_0 - 3K_1 + K_2)/128$, $J_9 = -(K_0 + K_1 - K_2)/128$, $J_{10} = K_2/128$, $J_{11} = -(K_0 - 3K_1 + 3K_2)/128$, $J_{12} = J_{13} = J_{14} = K_2/128$, $J_{15} = J_{16} = (K_0 + K_1 + K_2)/128$ and $J_{17} = J_{18} = -(2K_0 + 6K_1 + 3K_2)/128$.

The summations (1), (2), ..., (18) corresponding to the configurations indicated in Table 1.1 (see Ref. 23) are the sums which run over different sites, bonds and loops on the following cell:



A. Low temperature analysis

We propose a description of the ground states of the "Physical" three-dimensional model and to describe the low-temperature phase diagram in the space of the parameters T and h for certain values of the parameters K_0 ,

K_1 , K_2 and J in order to check the phase diagrams conjectured by Shnidman and Zia.

1. Ground states of the model

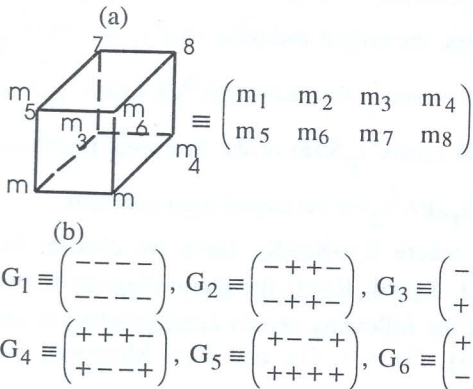
Our aim here is to determine all the periodic configurations of the lattice Z^3 that minimize the energy U (see the Appendix in Ref 23). For that, we divide the research of the ground states of the model on two stages:

1- The first stage consist in supposing that any translation-periodic ground state of the model is translation-invariant in every of eight sublattices of the lattice Z^3 and we consider by m_1, m_2, \dots, m_8 the parameters characterizing the magnetizations on the eight sublattices (Fig. 7a). Then we search, numerically, the values of the magnetizations (m_1, m_2, \dots, m_8) which minimize the energy U for given values of the parameters of the system.

2- The second stage consist in checking that there is no other ground states except those finding in the first stage; hence it is necessary to use correctly the definition of a ground state²¹: "A ground state is a periodic configuration such that any local perturbation increases its energy and then having a minimal energy". Therefore it is useful to look for the excitations (see below the definition of an excitation) of all the preceeding periodic configurations found in the first stage (see table 2 in Ref. 23). Hence we found that the values of all the excitations of all the states in the "supposed"-zero-phase diagrams are strictly positive and then by a definition, all the states found in this later are actually a ground states of the model (see Fig. 7b).

We only consider certain values of the parameters K_0 , K_1 , K_2 and J to describe the phase diagrams, at low temperature, if we vary the chemical potential, h , of the amphiphile component.

We denote by G_1 the "water" ground state (g.s), G_2 the set of "hexagonal" (infinite "rod" micelles), G_3 the set of "spherical" micelles, G_4 the set of mixed "rod-spherical" micelles, G_5 the set of mixed "rod-layer" micelles, G_6 the set of "reversed" micelles, G_7 the set of rarefied "spherical" micelles, G_8 the set of rarefied infinite "rod" micelles, G_9 the set of "lamellar" (infinite "bilayer" micelles), G_{10} the set of rarefied "reversed" micelles and G_{11} the amphiphile (see Fig. 7b).



$$G_7 \equiv \begin{pmatrix} - & - & - & - \\ - & - & - & + \\ - & - & - & + \\ - & - & - & + \end{pmatrix}, G_8 \equiv \begin{pmatrix} + & + & - & - \\ - & - & - & - \\ - & - & - & - \\ - & - & - & - \end{pmatrix}, G_9 \equiv \begin{pmatrix} + & + & + & + \\ - & - & - & - \\ - & - & - & - \\ - & - & - & - \end{pmatrix}$$

$$G_{10} \equiv \begin{pmatrix} + & + & + & + \\ + & + & + & - \\ + & + & + & - \\ + & + & + & - \end{pmatrix}, G_{11} \equiv \begin{pmatrix} + & + & + & + \\ + & + & + & + \\ + & + & + & + \\ + & + & + & + \end{pmatrix}.$$

FIG. 7: (a) (m_1, m_2, \dots, m_8) are the values of the spins on the eight sublattices. (b) Ground states of the model: G_1 the "water" ground state (g.s), G_2 the set of "hexagonal" (infinite "rod" micelles), G_3 the set of "spherical" micelles, G_4 the set of mixed "rod-spherical" micelles, G_5 the set of mixed "rod-layer" micelles, G_6 the set of "reversed" micelles, G_7 the set of rarefied "spherical" micelles, G_8 the set of rarefied infinite "rod" micelles, G_9 the set of "lamellar" (infinite "bilayer" micelles), G_{10} the set of rarefied "reversed" micelles and G_{11} the amphiphile.

Their energies, ϵ_0 , are

$$\begin{aligned} \epsilon_0(G_1) &= h, \epsilon_0(G_2) = -(K_1 + 2J)/2, \epsilon_0(G_3) = -(K_0 + 3J)/2, \\ \epsilon_0(G_4) &= -(2h + 3K_1 + K_0 + 9J)/8, \epsilon_0(G_5) = -(2h + K_1 + K_2 + 3J)/4, \\ \epsilon_0(G_6) &= -(2h + 3K_2 + 3J)/4, \epsilon_0(G_7) = -(6h + K_0 + 3J)/8, \\ \epsilon_0(G_8) &= -(2h + K_1 + 2J)/4, \epsilon_0(G_9) = -(K_2 + J)/2, \epsilon_0(G_{10}) \\ &= -3(2h + J + K_2)/8, \epsilon_0(G_{11}) = -h. \end{aligned} \quad (12)$$

2. The low temperature phase diagrams

We analysis 3 dimensional model with the theory of the first-order phase transition presented in Ref.19 and 20.

B. Mean field approach

Our motivation here is to provide, within the mean-field approximation, a description of the states of lowest free energy of the three-dimensional version of the model and to describe the phase diagrams in the space of the parameters T and h for certain values of the parameters K_0 , K_1 , K_2 and J characterising the interactions of the model. Then we check the conjectured phase diagrams proposed by Shnidman and Zia. So, for this study was the well-know fact that the chemical potential of the amphiphiles, h , for fixed values of the coupling interactions, may change the nature of phase transitions in fundamental way, inducing the appearance of multicritical points.

In mean field approximation the free energy, F , of the micellar binary solutions at three dimensions may be expressed as function of the inverse temperature β , variational parameters h_i , $i=1, \dots, 8$, the magnetizations m_i , $i=1, \dots, 8$, and J_i , $i=1, \dots, 18$, which are mentioned previously:

$$F = -\frac{1}{8\beta} \sum_{i=1}^8 \text{Log}(2\text{ch}(\beta h_i)) + \frac{1}{8} \sum_{i=1}^8 h_i m_i + U \quad (13)$$

where the function m_i , $i=1, \dots, 8$, that is the average magnetization per spin, is given as follows:

$$m_i = \tanh(\beta h_i)$$

The mean field equations in this situation are obtained by minimizing the expression of free energy, F , with respect to the variational parameters h_i , $i=1, \dots, 8$ which combined with the last expression of magnetization. Then the first equation of this system corresponding to m_1 is established in the Appendix in Ref.23.

The others mean field equations corresponding to m_2 , m_3 , ..., and m_8 must be obtained using the permutations indicate in the Appendix in Ref 23.

C. Results and discussion

In the case $K_0 > K_1 > K_2$ (here we choose, for example, $K_0=6J$, $K_1=3J$, $K_2=J$) the phase diagram shows the existence of the following phases corresponding to the ground states G_1 , G_3 and G_{11} which are defined previously. The tricritical point C separates the phase transition lines $L(-4.5, C)$ of the second order transition from one $L(C, 4.5)$ of the first order transition (Fig. 8).

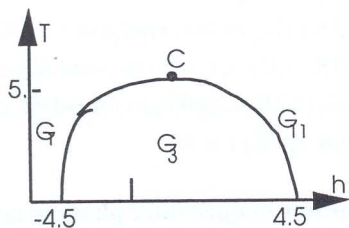


FIG. 8. Phase diagram of the model for $K_0 > K_1 > K_2$ (for example, $K_0=6J$, $K_1=3J$, $K_2=J$) on the T - h plane. Water (G_1), "spherical" micelles (G_3) and amphiphile (G_{11}) are the pure phases. The tricritical point C separates the phase transition lines $L(-4.5, C)$ of the second order transition from one $L(C, 4.5)$ of the first order transition.

In the case $K_1 > K_2 > K_0$ and $K_1 < 2K_2$ (here we choose, for example, $K_0=2J$, $K_1=6J$, $K_2=4J$) the phase diagram shows the existence of the following phases corresponding to the ground states G_1 , G_8 , G_2 , G_6 , G_{10} and G_{11} which are defined previously. Moreover, the critical end-point BA^2 separates the phase transition lines $L((A^3)_1, BA^2)$ and $L(BA^2, C_2)$ of the first order transitions from one $L(C_1, BA^2)$ of the second-order transition. The triple points $(A^3)_1$, and $(A^3)_2$ separate the phase transition lines $L(-4, (A^3)_1)$, $L((A^3)_1, BA^2)$, $L(C_1, (A^3)_2)$ and $L((A^3)_2, 7.5)$ of the first order transitions. The tricritical points C_1 and C_2 separate the phase transition lines $L(C_1, (A^3)_2)$ and $L(BA^2, C_2)$ of the first order transitions from ones $L(C_1, BA^2)$ and $L(C_2, .5)$ of the second-order transitions.

$L(C_1, BA^2)$ and $L(C_2, .5)$ of the second-order transitions.(Fig. 9).

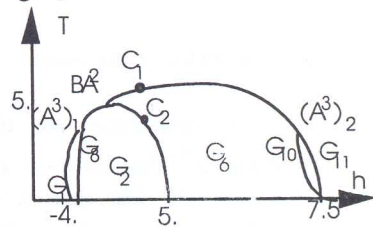


FIG. 9. Phase diagram of the model for $K_1 > K_2 > K_0$ (for example, $K_1 < 2K_2$, $K_0=2J$, $K_1=6J$, $K_2=4J$) on the T - h plane. Water (G_1), rarefied infinite "rod" micelles (G_8), "hexagonal" (infinite "rod" micelles) (G_2), "reversed" micelles (G_6), rarefied "renversed" micelles (G_{10}) and amphiphile (G_{11}) are the pure phases. The critical end-point BA^2 separates the phase transition lines $L((A^3)_1, BA^2)$ and $L(BA^2, C_2)$ of the first order transitions from one $L(C_1, BA^2)$ of the second-order transition. The triple points $(A^3)_1$, and $(A^3)_2$ separate the phase transition lines $L(-4, (A^3)_1)$, $L((A^3)_1, BA^2)$, $L(C_1, (A^3)_2)$ and $L((A^3)_2, 7.5)$ of the first order transitions. The tricritical points C_1 and C_2 separate the phase transition lines $L(C_1, (A^3)_2)$ and $L(BA^2, C_2)$ of the first order transitions from ones $L(C_1, BA^2)$ and $L(C_2, .5)$ of the second-order transitions.

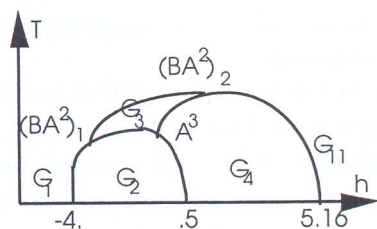


FIG. 11: Phase diagram of the model for $K_1 > K_0 > K_2$ (for example, $K_0=4J$, $K_1=6J$, $K_2=J$) on the T - h plane. Water (G_1), "hexagonal" (infinite "rod" micelles) (G_2), "spherical" micelles (G_3), mixed "rod-spherical" micelles (G_4) and amphiphile (G_{11}) are the pure phases. the critical end-point $(BA^2)_1$ and $(BA^2)_2$ separate the phase transition lines $L(-4, (BA^2)_1)$, $L((BA^2)_1, A^3)$, $L((BA^2)_2, A^3)$ and $L((BA^2)_2, 5.16)$ of the first order transitions from one $L((BA^2)_1, (BA^2)_2)$ of the second-order transition.

For the case where $K_1 > K_0 > K_2$ (here we choose, for example, $K_0=4J$, $K_1=6J$, $K_2=J$) the phase diagram shows the existence of the following phases corresponding to the ground states G_1 , G_2 , G_3 , G_4 , and G_{11} . Moreover, the

critical end-point $(BA^2)_1$ and $(BA^2)_2$ separate the phase transition lines $L(-4, (BA^2)_1)$, $L((BA^2)_1, A^3)$, $L((BA^2)_2, A^3)$ and $L((BA^2)_2, 5.16)$ of the first order transitions from one $L((BA^2)_1, (BA^2)_2)$ of the second-order transition (Fig. 11).

IV. CONCLUSIONS

We have presented some new theoretical and numerical results concerning the phase diagrams of the micellar binary solutions. We find that this model describes qualitatively the micellar phases observed experimentally¹³. Also, we check that the conjectured phase diagrams proposed by Shnidman and Zia is correct.

ACKNOWLEDGMENT

This work was supported by the PARS grant n°: physique 037

- ¹K. A Dawson and Z. Kurtovic, *J. Chem. Phys.* **92**, 5473 (1990)
- ²J. W. Halley. and A.J. Kolan, *J. Chem. Phys.* **88**, 3313 (1988)
- ³M. W. Matsen and D.E. Sullivan, *Phys. Rev. A* **41**, 2021 (1990)
- ⁴G. Gompper and M. Schick, *Chem. Phys. Lett.* **163**, 475 (1989)
- ⁵G. Gompper and M. Schick, *Self-Assembling Amphiphilic Systems in Phase Transitions and Critical Phenomena V. 16*, edited by C. Domb and J. L. Lebowitz (Academic, London, 1994)
- ⁶W. M. Gelbart, D. Roux and A. Ben-Shaul, *Micelles, Membranes, Microemulsions and monolayers*, (Springer-Verlag, New York, 1994)
- ⁷N. Jan and D. Stauffer, *J. Phys. France* **49**, 623 (1988)
- ⁸V. Degiorgio and M. Corti, *Physics of amphiphiles: Micelles, Vesicles and Microemulsions* (North-Holland, Amsterdam, 1985).
- ⁹G. J. T. Tiddy, *Phys. Rep.* **57**, 1 (1980)
- ¹⁰G. Gompper and S. Zschocke, *Europhys. Lett.* **16** 731 (1991)
- ¹¹J. M. Seddon, *Biochim. biophys. Acta.* **1031**, 1 (1990)
- ¹²H. Hoffmann, *Adv. Colloid Interface Sc.* **32**, 123 (1990)
- ¹³R. Strey, R. Schomäcker, D. Roux, F. Nallet and U. Olsson, *J. Chem. Soc. Faraday Trans.* **86**, 2253 (1990)
- ¹⁴V. Degiorgio, M. Corti and L. Cantu, *Chem. Phys. Lett.* **151**, 349 (1988)
- ¹⁵J. N. Israelachvili, D.J. Mitchell and B. W. Ninham, *J. Chem. Soc. Faraday Trans.* **72**, 1525 (1976)
- ¹⁶Y. Shnidman and R. K. P. Zia, *J. Stat. Phys.* **50**, 839 (1988)
- ¹⁷A. Benyoussef, L. Laanait and N. Moussa, *Phys. Rev. B* **48**, 16310 (1993)
- ¹⁸A. Benyoussef, L. Laanait, N. Masaif and N. Moussa, *J. Phys: Condens. Matter* **8**, 1 (1996)
- ¹⁹Ya. G. Sinai, *Theory of phase transitions: Rigorous Results* (Pergamon Press, London, 1982).
- ²⁰J. Slawny, in *Phase Transitions and Critical Phenomena V. 16*, edited by C. Domb and J. L. Lebowitz (Academic, London, 1987)
- ²¹J. Brimont, J. Slawny, *J. Stat. Phys.* **54**, 89 (1989).
- ²²R. B. Griffiths, *Phys. Rev. B* **12**, 345 (1975)
- ²³A. Benyoussef, L. Laanait, N. Masaif and N. Moussa, *J. Phys. : I France* **6**, 1043 (1996)